Eur. Phys. J. B **23**, 449–454 (2001)

THE EUROPEAN
PHYSICAL JOURNAL B
EDP Sciences

# High-pressure study of the non-Fermi liquid material $U_2Pt_2In$

P. Estrela[1], A. de Visser[1,a], T. Naka[1,2], F.R. de Boer[1], and L.C.J. Pereira[3]

[1] Van der Waals-Zeeman Institute, University of Amsterdam, Valckenierstraat 65, 1018 XE Amsterdam, The Netherlands
[2] National Research Institute for Metals, 1-2-1 Sengen, Tsukuba, Ibaraki 305-0047, Japan
[3] Department of Chemistry, Technological and Nuclear Institute, Apartado 21, 2686-953 Sacavém, Portugal

Received 2 March 2001 and Received in final form 29 June 2001

**Abstract.** The effect of hydrostatic pressure ($p \leq 1.8$ GPa) on the non-Fermi liquid state of $U_2Pt_2In$ is investigated by electrical resistivity measurements in the temperature interval 0.3–300 K. The experiments were carried out on single-crystals with the current along ($I \parallel c$) and perpendicular ($I \parallel a$) to the tetragonal axis. The pressure effect is strongly current-direction dependent. For $I \parallel a$ we observe a rapid recovery of the Fermi-liquid $T^2$-term with pressure. A comparison of the data with the magnetotransport theory of Rosch provides evidence for the location of $U_2Pt_2In$ at an antiferromagnetic quantum critical point. For $I \parallel c$ the resistivity increases under pressure, indicating the enhancement of an additional scattering mechanism.

**PACS.** 71.10.Hf Non-Fermi-liquid ground states, electron phase diagrams and phase transitions in model systems – 71.27.+a Strongly correlated electron systems; heavy fermions – 72.15.-v Electronic conduction in metals and alloys

## 1 Introduction

$U_2T_2X$ intermetallics, where T is a transition metal and X is In or Sn, have been the subject of intensive research, as this family of compounds may serve as an exemplary series to study the systematics of $5f$-electron hybridization [1]. The hybridization strength can be tuned by choosing the appropriate T and X elements, and as a result various ground states are observed, *e.g.* Pauli paramagnetism, local-moment antiferromagnetism and pronounced spin-fluctuating behaviour. Among the $U_2T_2X$ compounds, $U_2Pt_2In$ takes a special place, because: (i) it is a non-ordering heavy-electron compound with a strongly renormalized quasiparticle mass ($c/T = 0.41$ J/molU-K$^2$ at $T = 1$ K) [1] and (ii) it shows pronounced departures from the standard Fermi-liquid (FL) behaviour, or, in other words, it is a non-Fermi liquid (NFL) compound [2,3]. Currently, NFL compounds attract much attention [4–6], because NFL behaviour may be considered to represent a new ground state. In the case of $U_2Pt_2In$, the NFL properties are summarized by: (i) the specific heat varies as $c(T) \sim -T\ln(T/T_0)$ over almost two decades of temperature ($T = 0.1$–$6$ K) [2], (ii) the magnetic susceptibility shows a weak maximum at $T_{\rm m} = 8$ K for a magnetic field along the $c$ axis (tetragonal structure), while it increases as $T^{0.7}$ when $T \to 0$ for a field along the $a$ axis [3], and (iii) the electrical resistivity obeys a power law $T^{\alpha}$ with $\alpha = 1.25 \pm 0.05$ ($T < 1$ K) and $0.9 \pm 0.1$ ($T \to 0$), for the current along the $a$ and $c$ axis, respectively [7]. It is important to realize that $U_2Pt_2In$ is one of the rare stoichiometric (undoped) compounds which exhibits NFL behaviour at ambient pressure. This has the advantage that NFL properties can be examined without the need to apply mechanical pressure, like in $CePd_2Si_2$ and $CeIn_3$ [8], or chemical pressure, like in Ce(Cu, Au)$_6$ [6]. Other stoichiometric NFL compounds are $CeNi_2Ge_2$ [9], $CeCu_2Si_2$ [10], $YbRh_2Si_2$ [11] and $U_3Ni_3Sn_4$ [12,13].

The origin of the NFL behaviour in $U_2Pt_2In$ is still not settled, despite a thorough experimental characterization [7]. The most plausible scenarios are: (i) the proximity to a magnetic quantum critical point (QCP) and (ii) Kondo disorder. The QCP scenario is often discussed in terms of a simple Doniach-type of phase diagram [14]. Magnetic order emerges when the inter-site Ruderman-Kittel-Kasuya-Yosida (RKKY) interaction energy, given by $k_{\rm B}T_{\rm RKKY}$, starts to dominate the single-ion Kondo interaction energy, $k_{\rm B}T_{\rm K}$. By controlling the ratio $T_{\rm RKKY}/T_{\rm K}$ by varying the strength of the $f$-electron hybridization, the compound might be tuned to a magnetic QCP at $T = 0$. The QCP controls the physics over a wide range of temperatures, which results in NFL behaviour. Expressions for the low-temperature NFL term in the thermal, magnetic and transport properties of an itinerant (anti)ferromagnet, tuned to its quantum critical point, have been evaluated by Millis [15] and Rosch [16]. In the case of $U_2Pt_2In$, the QCP scenario is supported

---

[a] e-mail: `devisser@science.uva.nl`

by the notion that the compound is located at the non-magnetic side, close to the magnetic/non-magnetic borderline, in the Doniach-type phase diagram for the $U_2T_2X$ family of compounds [7,17]. The absence of magnetic order in $U_2Pt_2In$, at least down to $T = 0.05$ K, was recently demonstrated by $\mu$SR experiments [18], which put an upper bound of ~0.1 Oe on the internal field due to weak magnetic order.

The second possible explanation for NFL behaviour in $U_2Pt_2In$, is the presence of Kondo disorder [19]. Large disorder in a material may produce a distribution of Kondo temperatures. For each single-magnetic impurity the Kondo effect will take place at a different value of $T_K$. Averaging over such a distribution may result in thermodynamic and transport properties with NFL-like dependencies, due to the broad range of effective Fermi temperatures. Indeed, the residual resistivity values of $U_2Pt_2In$ are substantial [3], *i.e.* of the order of 100 $\mu\Omega$cm, which indicates considerable crystallographic disorder and/or defects. On the other hand, Rietveld analyses of the diffraction patterns obtained by single-crystal X-ray [3] and neutron-diffraction [20] yield good refinement factors and exclude significant Pt-In site inversion.

In this paper, we report on an investigation of the stability of the NFL phase of single-crystalline $U_2Pt_2In$ with respect to hydrostatic pressure. The electrical resistivity, $\rho(T)$, was measured for a current, $I$, along the $a$ and $c$ axis, up to pressures of 1.8 GPa. Here, we focus on the low-temperature data obtained for $I \parallel a$. At $p = 0$, $\Delta\rho \equiv \rho - \rho_0 \sim T^\alpha$ ($\rho_0$ is the residual resistivity) with $\alpha = 1.25 \pm 0.05$ for $T < 1$ K, whereas under pressure, the Fermi-liquid $T^2$ term is rapidly recovered. We have analysed the pressure dependence of the FL temperature interval within the theory of Rosch and provide evidence that $U_2Pt_2In$ is situated at or very close to an antiferromagnetic quantum critical point. For the analysis of the resistivity data with $I \parallel c$ is we refer to references [7,21].

## 2 Experimental

A single-crystalline batch of $U_2Pt_2In$ was prepared by a modified mineralization technique [22]. $U_2Pt_2In$ is a polymorphic compound, as was recently shown in reference [3]. Polycrystalline samples crystallize in the tetragonal $U_3Si_2$-type of structure (space group P4/mbm) with lattice parameters $a = 7.654$ Å and $c = 3.725$ Å, while single-crystalline material forms in the tetragonal $Zr_3Al_2$-type of structure (space group $P4_2$/mnm) with lattice parameters $a = 7.695$ Å and $c = 7.368$ Å. The $Zr_3Al_2$-type structure can be considered as a super-structure of the $U_3Si_2$-type of structure, with a doubling of the $c$-axis. Despite this polymorphism, significant differences in the electronic and magnetic properties of single- and polycrystalline samples have not been observed [7]. The residual resistivity values are large: $\rho_0$ equals 115 $\mu\Omega$cm and 210 $\mu\Omega$cm, for $I \parallel a$ and $I \parallel c$, respectively [3]. Since the resistivity at room temperature amounts to 220 $\mu\Omega$cm, low residual resistance ratio's $\rho_{RT}/\rho_0$ (where $\rho_{RT} \equiv \rho$ (300 K)) result: 1.9 and 1.1 for the $a$ and $c$ axis, respectively. The relative errors in these numbers amount to 10%, because of the uncertainty in the determination of the geometrical factor in the resistivity experiment. Transport experiments in a magnetic field lead to a reduction of $\rho_0$, which indicates that at least part of the high $\rho_0$-value is intrinsic and not due to defects and/or impurities [7].

The electrical resistivity of $U_2Pt_2In$ under pressure ($p \leq 1.8$ GPa) was measured for $I \parallel a$ and $I \parallel c$ in the temperature range 0.3–300 K. The resistivity was measured on bar-shaped or platelet-like samples using a standard low-frequency four-probe ac-technique with a typical excitation current of ~100 $\mu$A. The resistivity under pressure was measured using a copper-beryllium clamp cell. The samples were mounted on a specially designed plug and inserted into a teflon holder together with the pressure transmitting medium. A short tungsten carbide piston is used to transfer the pressure to the teflon holder. A mixture of Fluorinerts was used as pressure transmitting medium. The pressure values (accuracy 0.05 GPa) were calculated from the external load and corrected for an empirically determined efficiency of 80%. The pressure dependence of $\rho_{RT}$ was negligible. However, small changes in the geometrical factor (mainly in the distance between the voltage contacts) sometimes occurred. Therefore, at each pressure, the resistance curves were normalized to 1 at room temperature.

## 3 Results

The electrical resistivity $\rho_a(T)$ and $\rho_c(T)$ of $U_2Pt_2In$, normalized to 1 at 300 K, measured for $I \parallel a$ and $I \parallel c$, respectively, at zero pressure is shown in Figure 1a. The data measured under pressure are shown in Figure 1b, at the selected pressures of 0.2, 1.0 and 1.8 GPa. Hydrostatic pressure results in rather opposite effects for $I \parallel a$ and $I \parallel c$. For $I \parallel a$, pressure leads to an overall reduction of $\rho_a(T)$ and a recovery of the FL $T^2$ term at low temperatures (see Sect. 4), whereas for $I \parallel c$ $\rho_c(T)$ increases and develops a relative minimum at low temperatures ($T_{\min} \sim 4.8$ K at 1.8 GPa). The anisotropy in the resistivity of $U_2Pt_2In$ increases as a function of pressure. In Figure 2a, we show the low-temperature data taken in the interval 0.3–15 K for $I \parallel a$. For both current directions $\rho_0$ shows moderate changes as a function of pressure, which is another indication that the high $\rho_0$-values are not exclusively due to disorder.

The resistivity shows a weak maximum at $T_{\max} \sim 70$ K for $I \parallel a$ and ~100 K for $I \parallel c$. The pressure effect on $T_{\max}$ is strongly current-direction dependent: $T_{\max}$ shows a strong increase for $I \parallel a$, while it decreases slightly for $I \parallel c$. For $I \parallel a$ we suggest that the maximum is due to the formation of the Kondo-lattice, in which case $T_{\max}$ is proportional to the Kondo temperature $T_K$ [23].

The data shown in Figure 1b were taken on one and the same sample (#1), which had a platelet-like shape, such that the current could be applied along the $a$ and the $c$ axis. The zero-pressure data (Fig. 1a) for $I \parallel a$ were also measured on this sample, while the data for $I \parallel c$

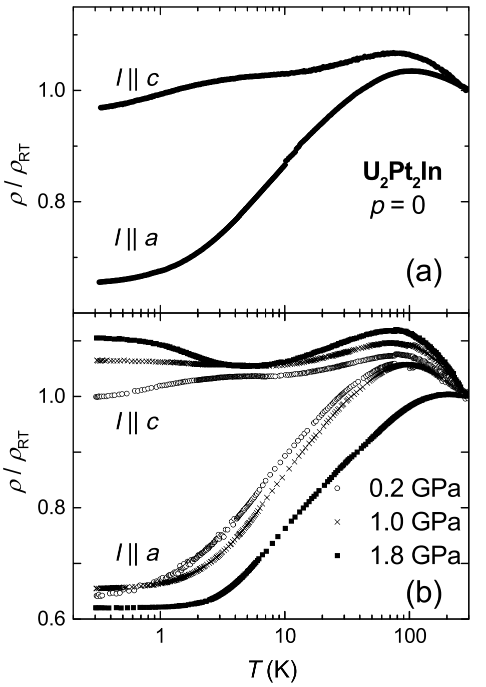

**Fig. 1.** Temperature dependence of the normalized resistivity of $U_2Pt_2In$ for $I \parallel a$ and $I \parallel c$: (a) at zero pressure and (b) under pressures as indicated. Notice the $\log T$ scale.

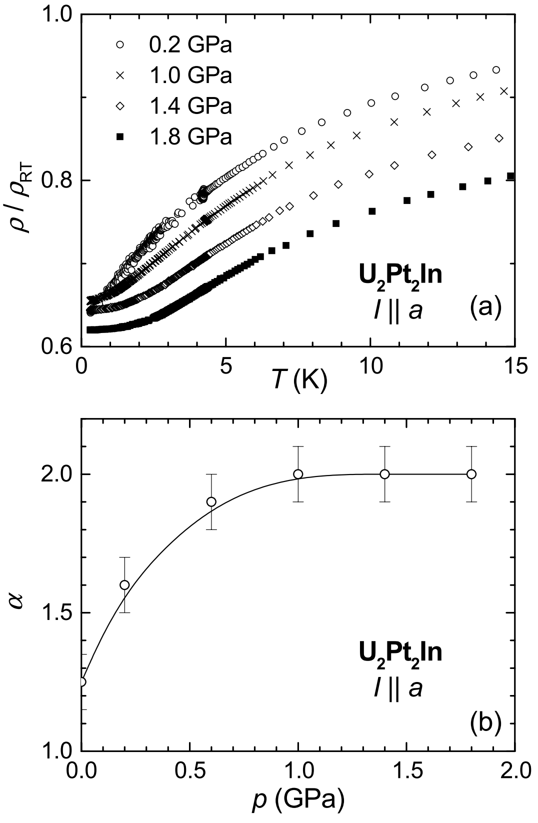

**Fig. 2.** (a) Low-temperature dependence of the normalized resistivity of $U_2Pt_2In$ for $I \parallel a$ at different pressures and (b) pressure dependence of the resistivity exponent $\alpha$ derived using equation (1). The solid line is to guide the eye.

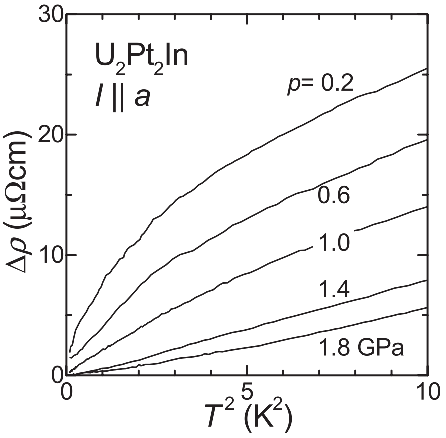

**Fig. 3.** Resistivity ($I \parallel a$) under pressure of $U_2Pt_2In$ in a plot of $\Delta\rho$ *versus* $T^2$.

were measured on a second crystal (sample #2). Measurements under pressure on other single crystals with $I \parallel c$ (sample #3) and with $I \parallel a$ (sample #4), confirm the overall behaviour: an increase of the transport anisotropy, the development of a low-temperature minimum in $\rho_c(T)$ and the recovery of a $T^2$ term in $\rho_a(T)$. Although all crystals were cut from the same single-crystalline batch, there is a weak sample dependence of some of the resistivity features, especially the values of $T_{min}$ are different for samples #1 and #3. For sample #1, the minimum develops near 1.0 GPa and attains a value of $T_{\rm min} \sim 4.8$ K at 1.8 GPa, while for sample #3, the minimum develops near 1.2 GPa and attains a value of $T_{\rm min} \sim 2.1$ K at 1.45 GPa [21].

## 4 Analysis

One of the main results of the pressure experiments is the recovery of the FL behaviour at moderate pressures for $I \parallel a$. We have analysed the low-temperature data in several ways. In the first method we express the resistivity as $\rho = \rho_0 + aT^\alpha$ and evaluate the exponent $\alpha$ by calculating

$$\alpha = 1 + \frac{\mathrm{d}\ln\left(\frac{\mathrm{d}\rho}{\mathrm{d}T}\right)}{\mathrm{d}\ln T} \cdot \qquad (1)$$

This method has the advantage that the uncertainty in the value of $\rho_0$ is eliminated. In fact, by computing $\alpha$ as a function of temperature with help of equation (1) an effective $\alpha_{\rm eff}(T)$ is obtained. At the lowest temperatures $\alpha_{\rm eff}(T)$ attains a constant value. The resulting values of $\alpha(p)$ for $T \to 0$ are shown in Figure 2b. At zero pressure $\alpha = 1.25 \pm 0.05$, but under pressure $\alpha$ increases and attains a value of $2.0 \pm 0.1$ at $p \sim 1.0$ GPa. At still higher pressures the value of $\alpha$ remains constant, while the Fermi-liquid temperature $T_{\rm FL}$ below which the $\Delta\rho \sim T^2$ is observed increases up to 1.5 K at the maximum pressure.

The second way of analysing the pressure data ($p \geq 0.2$ GPa) is by plotting $\Delta\rho$ as a function of $T^2$ (see Fig. 3). The data clearly show a strong increase of the $\Delta\rho \sim T^2$

regime with pressure. We have extracted $T_{\mathrm{FL}}$ by a least-squares fitting procedure. The pressure variation of $T_{\mathrm{FL}}$ is shown in Figure 4a (solid squares). Within the error bars, the data are consistent with $T_{\mathrm{FL}}$ being a linear function of pressure. The coefficient of the $T^2$ term amounts to $2.1 \pm 0.2$ $\mu\Omega\mathrm{cm/K}^2$ at 1.0 GPa and decreases to a value of $0.40 \pm 0.04$ $\mu\Omega\mathrm{cm/K}^2$ at 1.8 GPa. From these coefficients we can obtain a rough estimate for the electronic specific-heat coefficient by using the Kadowaki-Woods relation [24]. The resulting $\gamma$-values are $0.46 \pm 0.02$ J/molU-K$^2$ at 1.0 GPa and $0.20 \pm 0.01$ J/molU-K$^2$ at 1.8 GPa. The large $\gamma$-value at 1.0 GPa is in-line with the heavy-fermion description of $U_2Pt_2In$ and is of same order as the value of $c/T$ at 1 K (0.41 J/molU-K$^2$ [2]) at ambient pressure.

It is also of interest to compare the data with the magnetotransport theory of Rosch [16] for itinerant antiferromagnets in the paramagnetic regime close to a magnetic quantum critical point. In this model $T_{\mathrm{FL}}$ is calculated as a function of the distance (measured by the pressure) to the QCP and varies initially as $T_{\mathrm{FL}} = a_1(p - p_{\mathrm{c}})$ with a cross-over to $T_{\mathrm{FL}} = a_2(p - p_{\mathrm{c}})^{1/2}$ at higher distances, where $p_{\mathrm{c}}$ is the pressure at the QCP. The pressure ranges in which the different laws are observed depend on the amount of disorder $x$ in the system ($x \approx 1/\mathrm{RRR}$). For $I \parallel a$, we obtained $x \sim 0.6$, which indicates that our sample is in an (intermediate) regime of disorder. The model predicts in this case, that at the QCP, the temperature interval for the NFL $\Delta\rho \sim t^{3/2}$ law is strongly reduced, and that the low-temperature resistivity is dominated by a NFL $\Delta\rho \sim tx^{1/2}$ law. However, under pressure the FL behaviour $\Delta\rho \sim t^2 r^{-1/2}$ for $T \to 0$ becomes more and more dominant (here $r \propto (\delta - \delta_{\mathrm{c}})/\delta_{\mathrm{c}}$ measures the distance to the QCP in the paramagnetic phase). In Figure 4a we show the different NFL and FL regimes as deduced by fitting the resistivity under pressure to a $T^2$ term (see also Fig. 3) at the lowest temperatures and a term linear in $T$ at higher temperatures. An example (at 1.8 GPa) of the quality of such a fit is shown in Figure 4b. Figure 4a shows that the data are consistent with $T_{\mathrm{FL}}$ being a linear function of pressure with $p_{\mathrm{c}} = 0$. The cross-over to a $T_{\mathrm{FL}} = a_2(p - p_{\mathrm{c}})^{1/2}$ dependence (dashed line in Fig. 4a) is expected near 3.0 GPa. The $\Delta\rho \sim T$ region is predicted to occur in the reduced temperature range $x < T/\Gamma < x^{1/2} (x < 1)$, where $\Gamma$ defines the temperature scale where the spin fluctuations are destroyed ($\Gamma \sim T_{\mathrm{K}}$ or $T_{\mathrm{coh}}$). From Figure 4a we extract that the $\Delta\rho \sim T$ region is found in the temperature range 2.8–4.7 K, from which it follows $x = 0.34$ and $\Gamma = 8.1$ K. The agreement between the calculated value $x = 0.34$ and the experimental value $x \sim 0.6$ ($= 1/RRR$) is, given the rather simple data treatment, satisfactory. Notice that $\Gamma$ is about equal to $T_{\mathrm{m}}$, *i.e.* the temperature of the maximum in the susceptibility. The temperature-pressure diagram presented in Figure 4a is consistent with the scaling diagram for the resistivity presented by Rosch. However, a value of the exponent $\alpha = 3/2$ predicted at the lowest temperatures at the QCP is not observed. Instead we find $\alpha = 1.25$ at $p = 0$ and $1 < \alpha < 2$ for non-zero pressures. This is possibly due to the fact that under pressure the $\Delta\rho \sim t^{3/2}$ regime becomes very small and a proper analysis is hampered by cross-over effects. We conclude that the analysis of the resistivity data within the model of Rosch yields additional support for $U_2Pt_2In$ exhibiting an antiferromagnetic QCP at zero pressure.

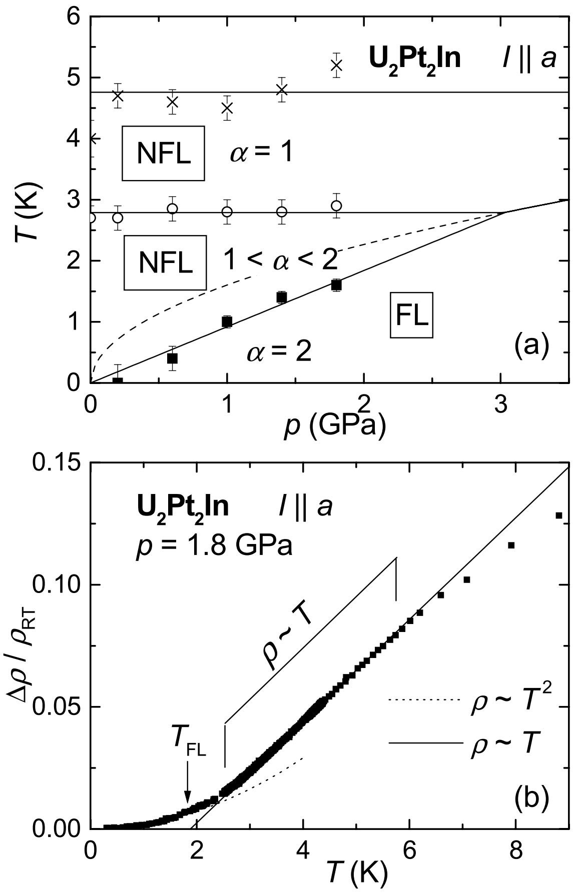

**Fig. 4.** (a) Pressure dependence of $T_{\mathrm{FL}}$ (closed squares) and of the temperature range in which $\rho \sim T$ (between (o) and (x)). The meaning of the dashed line is explained in the text. (b) Temperature variation of $\Delta\rho/\rho_{\mathrm{RT}}$ for $U_2Pt_2In$ at $p = 1.8$ GPa. The dashed and solid lines show the behaviour $\rho \sim T^2$ and $\rho \sim T$.

For the electrical resistivity measured for $I \parallel c$ the situation is different. At zero-pressure $\Delta\rho_{\mathrm{c}} \sim T^{\alpha}$ with $\alpha \sim 0.9 \pm 0.1$ for $T \to 0$. Under pressure $\alpha$ first increases, but near 1.0 GPa $\rho_{\mathrm{c}}(T)$ develops a minimum, which becomes more pronounced with increasing pressure. This behaviour, first observed on sample #3, was reported in reference [21]. Measurements of $\rho_{\mathrm{c}}(T)$ at $p = 1.8$ GPa in a magnetic field applied along the current direction show a suppression of $T_{\min}$ from ~4.8 K at zero field to ~2.2 K in a field of 8 T, which indicates a magnetic nature of the minimum (see also Ref. [21] for data on sample #3). Clearly, for $I \parallel c$ the magnetotransport theory of Rosch does not apply.

## 5 Discussion

The pressure dependence of the electrical resistivity of $U_2Pt_2In$ for $I \parallel a$ as measured up to 1.8 GPa provides evidence for an antiferromagnetic quantum phase transition at $T = 0$. At low temperatures, pressure results in the recovery of the FL regime. The data are in reasonable agreement with the transport theory of metals near an antiferromagnetic QCP model proposed by Rosch. The pressure-induced shift of $T_{\max}$ at high temperatures can be attributed to the usual increase of the Kondo temperature. The increase of $T_K$ reflects a stronger conduction electron – $f$-electron hybridization and, therefore, the exchange parameter $J$ increases. This is in agreement with the appearance of the FL $\Delta\rho \sim T^2$ behaviour at low temperatures.

An attractive method to probe the QCP scenario further is by expanding the lattice of $U_2Pt_2In$ through alloying with *e.g.* Th, which should result in magnetic order. From the change of the lattice constants in the pseudoternary series $(U_{1-x}Th_x)_2Pt_2In$ [25], we calculate a negative chemical pressure of –0.2 GPa per at.% Th doping. Thus for $x = 0.1$, the negative chemical pressure amounts to –2 GPa, which should lead to an ordering temperature in the range 15–20 K. Resistivity studies on polycrystalline $(U_{1-x}Th_x)_2Pt_2In$ samples reported in the literature [26], indicate that the resistivity at low temperatures ($T > 1.5$ K) gradually changes from $\Delta\rho \sim T$ towards $\Delta\rho \sim T^2$ as the Th content increases. For $x = 0.1$ the resistivity data show a change of slope near 19 K, which possibly indicates magnetic ordering. However, the change of slope might also be due to small amounts of impurity phases, like UPt, which has two magnetic phase transitions at 27 K and 19 K [27]. Specific-heat measurements carried out on polycrystalline $(U_{1-x}Th_x)_2Pt_2In$ ($0 \leq x \leq 0.1$) [28] do not show any evidence for magnetic order down to 2 K. On the other hand, $\mu$SR experiments do signal magnetic transitions in some of the samples [7]. These conflicting results evoke the need for high-quality single-phase material. Also, it should be noticed that substitution of U by Th dilutes the $f$-electron lattice, which might impede the emergence of magnetic order.

Although the analysis of the resistivity ($I \parallel a$) of $U_2Pt_2In$ under pressure is consistent with an antiferromagnetic QCP in 3D, the specific heat, $c/T \sim -\ln(T/T_0)$, measured in the $T$ range 0.1–6 K, is possibly indicative for a ferromagnetic QCP. However, a diverging $T \ln T$ term in the specific heat is a general feature of a system with a dimension $d$ equal to the dynamical critical exponent $z$. Possibly, quasi-two dimensional fluctuations could lead to a reduction of $d$ and $z$, like for the NFL compound $CeCu_{5.9}Au_{0.1}$, which is located at an antiferromagnetic QCP and for which it has been proposed $d \approx z \approx 2.5$ [6]. On the other hand, it cannot be excluded that the specific heat shows a cross over to the $c/T = \gamma_0 + aT^{1/2}$ behaviour derived [15] for an antiferromagnetic QCP below $T = 0.1$ K. Clearly, experiments at lower temperatures are needed to settle this issue.

The rapid recovery of the FL behaviour under pressure as probed by the resistivity data for $I \parallel a$ does not yield support for Kondo-disorder as mechanism for NFL behaviour in $U_2Pt_2In$. Since the compressibility is isotropic [7] pressure is expected to result in the further broadening of the distribution of Kondo-temperatures and thus the concurrent NFL behaviour is preserved.

The strong current-direction dependence of the pressure effect is unusual. At zero pressure the data indicate a significant anisotropy of the Fermi surface. Under pressure this anisotropy becomes even stronger. The emergence of a low-temperature minimum in the resistivity for $I \parallel c$ is not understood.

## 6 Conclusions

We have investigated the effect of hydrostatic pressure ($p \leq 1.8$ GPa) on the non-Fermi liquid state of $U_2Pt_2In$, by means of electrical resistivity experiments in the temperature interval 0.3–300 K. The experiments carried out on single-crystals show that the pressure effect depends strongly on the current direction. For $I \parallel a$, the low-temperature resistivity at zero pressure shows a NFL power law behaviour, $\rho \sim T^\alpha$, with $\alpha = 1.25 \pm 0.05$. Under pressure the NFL behaviour is suppressed: $\alpha$ increases and attains the FL value of $2.0 \pm 0.1$ at $p \sim 1.0$ GPa. A comparison of the data for $I \parallel a$ with the magnetotransport theory of Rosch provides evidence for the location of $U_2Pt_2In$ at an antiferromagnetic quantum critical point. For $I \parallel c$ the behaviour is complex and the data suggest the enhancement under pressure of an additional component to the resistivity.

P.E. acknowledges the European Commission for a Marie Curie Fellowship within the TMR program. T.N. thanks A. Matsushita for assistance in developing the high-pressure cell. AdV acknowledges support within ESF/FERLIN programme.

## References

1. L. Havela, V. Sechovský, P. Svoboda, M. Diviš, H. Nakotte, K. Prokeš, F.R. de Boer, A. Purwanto, R.A. Robinson, A. Seret, J.M. Winand, J. Rebizant, J.C. Spirlet, M. Richter, H. Eschrig, J. Appl. Phys. **76**, 6214 (1994).
2. P. Estrela, A. de Visser, F.R. de Boer, G.J. Nieuwenhuys, L.C.J. Pereira, M. Almeida, Physica B **259-261**, 409 (1999).
3. P. Estrela, L.C.J. Pereira, A. de Visser, F.R. de Boer, M. Almeida, M. Godinho, J. Rebizant, J.C. Spirlet, J. Phys. Cond. Matt. **10**, 9465 (1998).
4. *Proceedings of ITP Workshop on Non-Fermi-Liquid Behaviour in Metals (Santa Barbara)*, J. Phys. Cond. Matt. **8**, 9675–10148 (1996).
5. P. Coleman, Physica B **259-261**, 353 (1999).
6. H.v. Löhneysen, J. Magn. Magn. Mater. **200**, 532 (1999).
7. P. Estrela, Ph.D. thesis, University of Amsterdam, 2000.
8. N.D. Mathur, F.M. Grosche, S.R. Julian, I.R. Walker, D.M. Freye, R.K.W. Haselwimmer, G.G. Lonzarich, Nature **394**, 39 (1998).

9. P. Gegenwart, F. Kromer, M. Lang, G. Sparn, C. Geibel, F. Steglich, Phys. Rev. Lett. **82**, 1293 (1999).
10. F. Steglich, P. Gegenwart, C. Geibel, P. Hinze, M. Lang, C. Langhammer, G. Sparn, O. Trovarelli, Physica B **280**, 349 (2000).
11. O. Trovarelli, C. Geibel, C. Langhammer, S. Mederle, P. Gegenwart, F.M. Grosche, M. Lang, G. Sparn, F. Steglich, Physica B **281-282**, 372 (2000).
12. L. Shlyk, P. Estrela, J.C. Waerenborgh, L.E. De Long, A. de Visser, D.P. Rojas, F. Gandra, M. Almeida, Physica B **292**, 89 (2000).
13. P. Estrela, A. de Visser, F.R. de Boer, T. Naka, L. Shlyk, Phys. Rev. B **63**, 212409 (2001).
14. S. Doniach, Physica B **91**, 231 (1977).
15. A.J. Millis, Phys. Rev. B **48**, 7183 (1993).
16. A. Rosch, Phys. Rev. B **62**, 4945 (2000).
17. V.H. Tran, Z. Zolnierek, A.J. Zaleski, H. Noël, Solid State Commun. **101**, 709 (1997).
18. P. Estrela, A. de Visser, G.J. Nieuwenhuys, A. Amato, A. Schenck, L.C.J. Pereira, to be published.
19. E. Miranda, V. Dobrosavljevic, G. Kotliar, J. Phys. Cond. Matt. **8**, 9871 (1996).
20. A. Martin-Martin, L.C.J. Pereira, G.H. Lander, J. Rebizant, F. Wastin, J.C. Spirlet, P. Dervenagas, P.J. Brown, Phys. Rev. B **59**, 11818 (1999).
21. P. Estrela, T. Naka, A. de Visser, F.R. de Boer, L.C.J. Pereira, M. Almeida, Physica B **281-282**, 381 (2000).
22. L.C.J. Pereira, Ph.D. thesis, University of Lisbon (1998).
23. A. Yoshimori, H. Kasai, J. Magn. Magn. Mater. **31-34**, 475 (1983).
24. K. Kadowaki, S.B. Woods, Solid State Commun. **58**, 507 (1986).
25. L.C.J. Pereira, J.C. Waerenborgh, I. Catarino, G. Bonfait, M. Godinho, M. Almeida, J. Alloys Compounds **317-318**, 419 (2001).
26. A.M. Strydom, P. de V. du Plessis, Physica B **230-232**, 62 (1997).
27. P.H. Frings, J.J.M. Franse, J. Magn. Magn. Mater. **51**, 141 (1985).
28. I. Catarino, L.C.J. Pereira, J.C. Waerenborgh, M. Almeida, M. Godinho, G. Bonfait, J. Magn. Magn. Mater. **226-230**, 92 (2001).